Journal of Atomic, Molecular, Condensate & Nano Physics
Vol. 6, No. 3, pp. 183–189, 2019
ISSN 2349-2716 (online); 2349-6088 (print)
Published by RGN Publications

http://www.rgnpublications.com

DOI: 10.26713/jamcnp.v6i3.1292

Study of Effects of Hot Phonon on Hot Electron Transport

Research Article

Tarun Kumar Dey[1] and Randhir Kumar[2,*]

[1] *Post Graduate Department of Physics, L. S. College* (*B.R.A. University*), *Muzaffarpur 842 001, Bihar, India*
[2] *Department of Physics, J. P. University, Chapra 841 301, India*
***Corresponding author:** krandhir782@gmail.com

Abstract. We study the influence of hot phonons on hot electron transport within the drain region is investigated. The ensemble *Monte Carlo* (MC) method self-consistently coupled with Poisson's equation is used. This MC simulation is three-dimensional in k-space and two-dimensional in real space. The two-dimensional model is possible if physical quantities have no significant variation along the third direction. The phonon *Boltzmann transport equation* (BTE) is solved and the mean heat generation rate is calculated.

Keywords. Hot electron; Monte Carlo simulation; Phonon population

PACS. 05.60.Gg

Received: September 11, 2019 **Accepted:** November 18, 2019

1. Introduction

Modern semiconductor devices already operate at lengths comparable to the electron's mean free path at room temperature [1, 2], and future novel devices will continue to advance further in this regime. At such length scales, ballistic transport of carriers will be dominant within the device channel. Carrier scattering is suppressed and generation of hot electrons will be significant in the drain region. Scatterings of these hot electrons altogether impact the channel current [3]. It is well known that the localized phonon emission from hot electrons near drain is the source of heat generation in the device. The dimension of this heat source is expected to be of the order of a few nanometers. When these hot electrons collide with the semiconductor lattice, hot phonons are produced, causing an extremely high rate of

heat generation. Hot phonons can occur in an extended, essentially homogeneous, region in bulk semiconductor or in a two-dimensional heterolayer [4]. Hot phonon effects, both in bulk semiconductors and microstructures, have been investigated by several authors [5, 6]. Hot phonon emission can effectively disturb the phonon distribution in thermal equilibrium. The hot and non-equilibrium phonon problems have been the subject of considerable interest over last few years. Understanding the problem is essential for solving the self-heating and reliability issues in nanoscale and thin-film transistors. Hot phonons (mainly longitudinal optical (LO) phonons) dramatically affect the electron transport in small-scale semiconductor structures, e.g. the high-field electron transport in semiconductor quantum wells, wires and resonant hetero-structure tunneling diodes [7, 8]. Most of the previous researches in this area are basically concentrated on influence of hot phonons on the electron energy relaxation after initial electro- or photo-excitation.

In this work, the influence of hot phonons on hot electron transport within the drain region is investigated. This MC method has been described in greater detail in previous works [9, 10]. The phonon *Boltzmann transport equation* (BTE) is solved and the mean heat generation rate is calculated. The simulation compares the results of two cases:
Case 1: The non-equilibrium that is actually present around the drain edge is neglected.
Case 2: The non-equilibrium phonon-occupation conditions are correctly considered at drain edge.

Our result shows that the mean electron energy within the drain is larger when the non-equilibrium conditions are correctly considered (Case 2). Heat generation, mean electron velocity and drain current are all estimated to have lower values if the non-equilibrium conditions are considered. We argue that the increase of the hot phonon population and the hot-phonon re-absorption rate are main reasons for these results.

2. Simulation Method

A bulk silicon n^+-i-n^+ diode along the [11] direction, as shown in Figure 1, is used for simulation purpose. The lengths of the source, channel, and drain are 100, 40 and 100 nm, respectively and diode width is 40 nm. Doping concentrations of the source and drain are set to $ND = 5 \times 10^{20}\,\mathrm{cm}^{-3}$. The channel is assumed to be both intrinsic and ballistic at lattice temperature of 300 K. The electrostatic potential is updated every 2 fs using Poisson's equation. The band structure is modeled using the non-parabolic band approximation, including the six conduction X-valleys of silicon [12]. The non-parabolicity factor α is set to $0.5\,\mathrm{eV}^{-1}$. The low device voltage ranges means that impact ionization and other high-energy scatterings can be neglected. The intravalley acoustic and intervalley phonon scattering are considered within the source and drain region [13, 14]. Since in this work we intend to explore the details of the hot phonon generation, all phonon scattering events are assumed inelastic, and the electrons exchange energy with the lattice are determined by the phonon dispersion and scattering selection rules. For simplicity, the carrier-carrier scattering, ionized impurity scattering and roughness scattering are not taken into account. Scatterings are treated in the standard way utilizing Fermi's Golden Rule. The respective forms of the scattering rates for the intravalley and intervalley phonon scattering are given by eq. (1) and eq. (2), respectively [15].

$$W(k) = \frac{\pi D_{ij}^2 Z_{ij}}{\rho \omega_{ij}} \left(N_q(T) + \frac{1}{2} \mp \frac{1}{2} \right) N\left(E_k \pm \hbar\omega_{ij}\right); \tag{1}$$

$$W(k) = \frac{\Xi^2 m_d}{4\pi\rho\hbar^2 k_s} \int \frac{1}{\omega_q} \left(N_q(T) + \frac{1}{2} \mp \frac{1}{2} \right) I_q q^3 dq \,, \tag{2}$$

where ρ is the mass density of the material, Ξ is the deformation potential including Ξ_{LA} and Ξ_{TA}, m_d is the density-of-states effective mass, I_q is the overlap integral of the wave function, Z_{ij} is the number of possible equivalent final valleys of the same type, D_{ij} is the coupling constant, $\hbar\omega_{ij}$ is the corresponding phonon energy, and ω is the phonon frequency. Here for f-type scattering, $Z = 4$, and for g-type scattering $Z = 1$ for bulk silicon. The values for the effective scattering deformation potentials are extracted from ref. [16]. The upper and lower signs compare to the phonon ingestion and phonon discharge forms, individually. N_q is the average phonon occupation number given by the Bose-Einstein distribution. Under equilibrium conditions, $N_q(T) = [\exp(\hbar\omega_q/k_B T) - 1]^{-1}$. Under non-equilibrium conditions, N_q must be determined by solving the BTE.

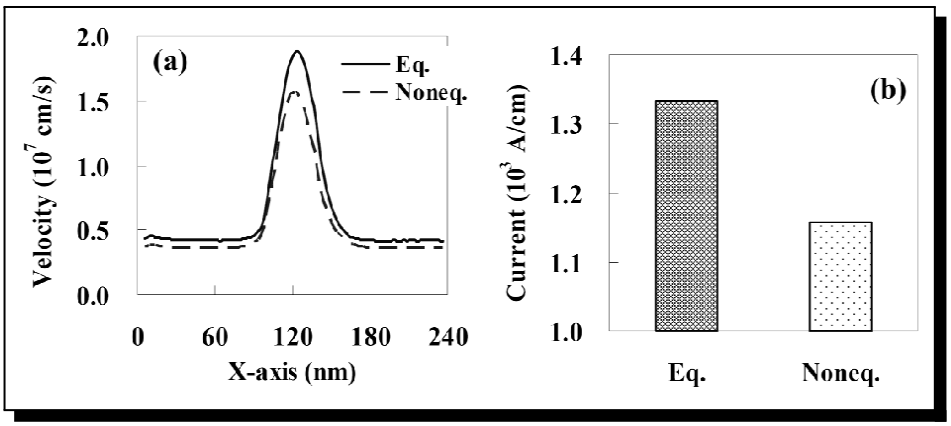

Figure 1. (a) Distribution of the mean velocity of electrons along the X-axis, and (b) the drain current at $VD = 0.3$ V for the equilibrium and non-equilibrium phonon occupation cases

Intravalley acoustic phonon scatterings were treated individually and the phonon frequency dependence on the wave vector were taken into account. Each branch of the acoustic phonon dispersion was modeled with the analytical approximation [16]. For intervalley phonon scattering, the numerical values of the phonon energies for the three g-types and for the three f-types are similar to those shown in ref. [17]. The phonon dispersion is also used when computing the final electron state after considering both momentum and energy conservation. The mean heat generation rate can be obtained from eq. (2)

The non-equilibrium phonon occupation number dominates the transport near the hotspots within the drain region and is determined by solving the phonon BTE in the relaxation-time approximation given by:

$$\left.\frac{\partial N_q}{\partial t}\right|_{ph-ph} = -\frac{N_q - N_q(T)}{\tau_{ph}}, \tag{3}$$

where τ_{ph} is the phonon lifetime, which is assumed to be equal for all values of q, N_q is the non-equilibrium phonon occupation, and $N_q(T)$ is the equilibrium phonon occupation at the lattice temperature T. Several theoretical approaches for the solution of eq. (3) have been presented in the literature. Details of the various methods can be found in ref. [18]. For all optical modes, a lifetime in the order of 10 ps can be assumed [19]. The lifetime of zone-center

optical modes in silicon at room temperature is almost on the same order as well. This time is long enough to assume semi-equilibrium, and hence the right side of eq. (3) can be equaled to zero. The phonons do not simply decay and disappear from the system; they are also created via emission from hot electrons. By introducing this factor and then rewriting eq. (3), the phonon occupation number can be expressed as [15]

$$N_q = Q''' \frac{n}{N_{\text{sup}}} \frac{6\pi^2}{q_{\text{max}}^3} \frac{\tau_{ph}}{t_{\text{sim}}} + N_q(T), \tag{4}$$

where Q''' is the sum of the generated phonon energy at the last time step t_{sim}, n is the doping concentration, and q_{max} is the maximum wave vector of the carriers.

To clarify the role of hot phonons inside the drain region, the simulation is performed under different conditions in the source, channel and drain regions. The channel is assumed to be completely ballistic. The intravalley acoustic, three g-type, and three f-type intervalley phonon scatterings are considered in the source region for all simulations. For the drain region, only the intervalley g-LO phonon scattering is considered under the equilibrium and non-equilibrium phonon occupation conditions, respectively.

3. Results and Discussion

Figure 1(a) shows the distribution of the mean electron velocity along the X-axis and Figure 1(b) shows the drain current under both equilibrium and non-equilibrium phonon occupation conditions. When the non-equilibrium phonon occupation is considered, the simulation results for the mean electron velocity and drain current are lower than equilibrium condition. We propose that the hot phonon population and the change in phonon occupation rates are the main reasons for these results. As the number of hot electrons in the drain region increases, hot phonon will also increase because the emission rate is larger than the absorption rate of the intervalley g-LO phonons. Thus, the phonon equilibrium condition is disturbed and the non-equilibrium phonon occupation increases, as shown in Figure 2. In this case, the absorption rate of the g-LO phonon is increased and the values are larger than those under the equilibrium condition.

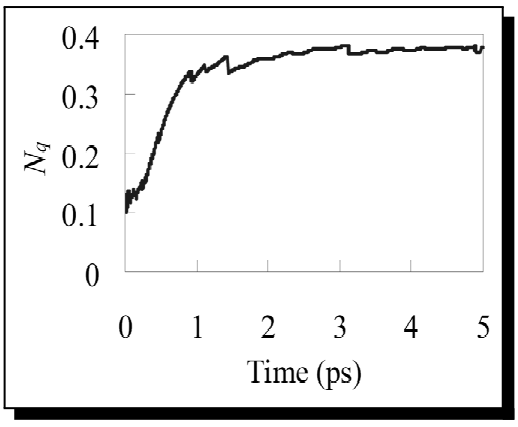

Figure 2. Phonon occupation versus time for non-harmony conditions

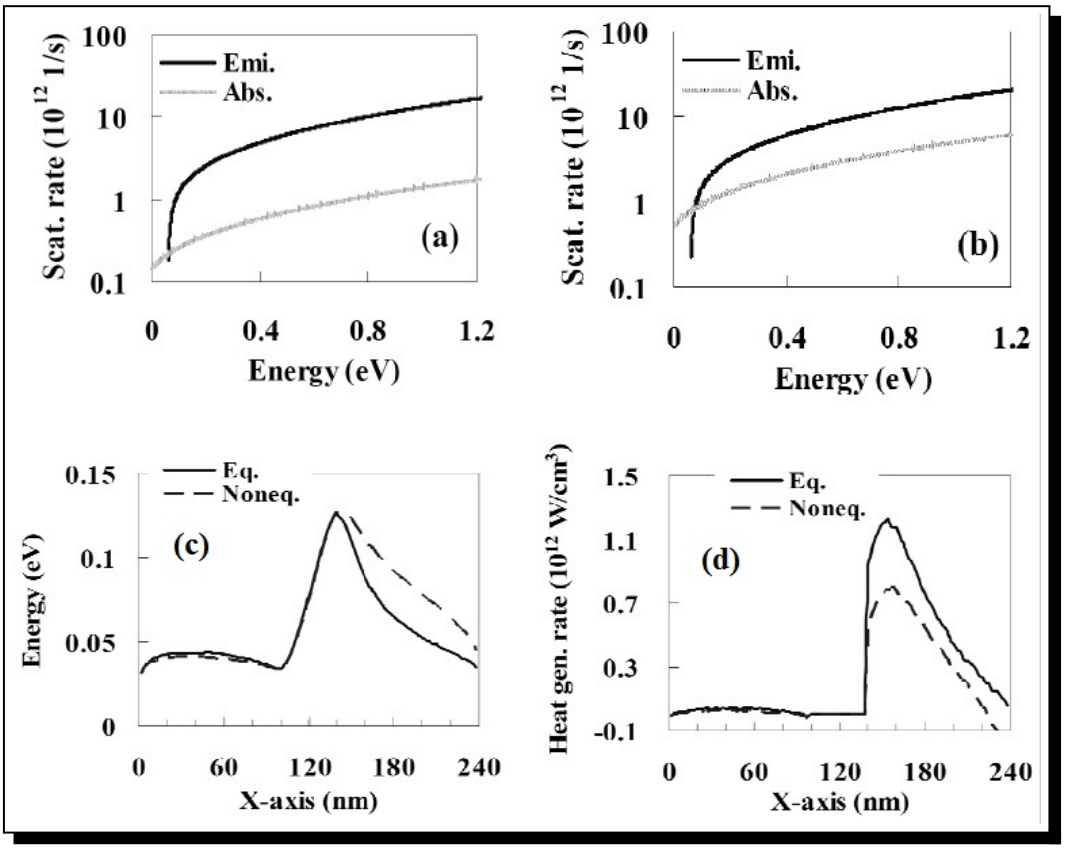

Figure 3. (a) Total scattering rates for g-LO phonon scattering under, (b) equilibrium condition (N_q = 0.0945), (c) non-equilibrium condition (N_q = 0.36), respectively. $\hbar\omega$ = 61 meV, T = 300 K, V_D = 0.3V and (c) Dispersion of mean vitality of electrons, (d) mean rate of heat age along the X-pivot in a ballistic channel diode at V_D = 0.3 V for cases that: the balance (strong line) and non-equilibrium phonon (dashed line) occupation conditions are considered in the channel

Therefore, the mean electron energy within the drain region under the non-equilibrium condition is larger than equilibrium condition, as shown in Figure 3(a). It should be noted that the emission rate of the g-LO phonon is almost unchanged. Figure 3(b) shows that the heat generation within the drain region is smaller for non-equilibrium phonon effect case. Figure 3(c) and 3(d) shows the depression of mean velocity of electrons and mean rate of heat age along the x-pivot in a ballistic channel diode. Intervalley g-LO phonon scattering is isotropic scattering, and has the same scattering probability in any direction. Considering the results above, it can be concluded that for non-equilibrium case when hot phonon generation is dominated within the drain region, the hot electrons have higher possibility of scattering in the source direction with high energy. This will increase the flow of electrons in reverse direction and degrade the mean electron velocity and drain current.

4. Conclusion

In this work, we investigated the influence of hot phonon distribution on the hot electron transport within the drain region of a ballistic channel diode, by implementing a Monte Carlo method equipped with the analytical electronic band and the phonon dispersion. The mean electron velocity and the drain current are degraded as the non-equilibrium phonon occupation

at the drain edge increases. These results are explained by the non-equilibrium g-LO phonon distribution caused by the high re-absorption rate of phonons and the low heat generation within the drain region. The surplus hot electrons are rebounded from the drain region and are transported toward source with high energy and velocity. We conclude that the hot phonon effect should not be neglected in the study of hot electron transport within the drain region if the hot phonon generation is significantly increased.

Competing Interests

The authors declare that they have no competing interests.

Authors' Contributions

All the authors contributed significantly in writing this article. The authors read and approved the final manuscript.

References

[1] Y. S. Ju and K. E. Goodson, Phonon scattering in silicon films with thickness of order 100 nm, *Appl. Phys. Lett.* **74**(20), 3005 (1999), DOI: 10.1063/1.123994.

[2] A. Svizhenko and M. P. Anantram, Role of scattering in nanotransistors, *IEEE Trans. Electron Devices* **50**, 1459 (2003), DOI: 10.1109/TED.2003.813503.

[3] W. Pötz and P. Kocevar, Electronic power transfer in pulsed laser excitation of polar semiconductors, *Phys. Rev. B* **28**, 7040 (1983), DOI: 10.1103/PhysRevB.28.7040.

[4] D. Y. Oberli, G. Böhm and G. Weimann, Role of interface optical phonons in cooling hot carriers in GaAs-AlAs quantum wells, *Phys. Rev. B* **47**, 7630 (1993), DOI: 10.1103/PhysRevB.47.7630.

[5] N. S. Mansour, Y. M. Sirenko, K. W. Kim, M. A. Littlejohn, J. Wang and J. P. Leburton, Carrier capture in cylindrical quantum wires, *Appl. Phys. Lett.* **67**, 3480 (1995), DOI: 10.1063/1.115253.

[6] S. Koch, T. Waho and T. Mizutani, InGaAs resonant tunneling transistors using a coupled-quantum-well base with strained AlAs tunnel barriers, *IEEE Trans. Electron Devices* **41**, 1498 (1994), DOI: 10.1109/16.310099.

[7] K. Kurishima, H. Nakajima, T. Kobayashi, Y. Matsuoka and T. Ishibashi, Fabrication and characterization of high-performance InP/InGaAs double-heterojunction bipolar transistors, *IEEE Trans. Electron Devices* **41**, 1319 (1994), DOI: 10.1109/16.297724.

[8] K. Tomizawa. *Numerical Simulation of Submicron Semiconductor Devices*, Artec House, London (1993).

[9] M. Lundstrom, *Fundamentals of Carrier Transport*, Cambridge University Press (2000).

[10] C. Jacoboni and L. Reggiani, The Monte Carlo method for the solution of charge transport in semiconductors with applications to covalent materials, *Rev. Mod. Phys.* **55**, 645 (1983), DOI: 10.1103/RevModPhys.55.645.

[11] C. Hamaguchi, Quantum structures, in *Basic Semiconductor Physics*, Springer (2001), DOI: 10.1007/978-3-662-04656-2_8.

[12] E. Pop, R. W. Dutton and K. E. Goodson, Analytic band Monte Carlo model for electron transport in Si including acoustic and optical phonon ispersion, *J. Appl. Phys.* **96**, 4998 (2004), DOI: 10.1063/1.1788838.

[13] W. Cai, C. M. Marchetti and M. Lax, Nonequilibrium phonon effect on time-dependent relaxation of hot electrons in semiconductor heterojunctions, *Phys. Rev. B* **35**, 1369 (1987), DOI: 10.1103/PhysRevB.35.1369.

[14] Ole Christian Norum, *Monte Carlo Simulation of Semiconductors–Program Structure and Physical Phenomena*, Master's Thesis, Norwegian University of Science and Technology, (2009), `http://hdl.handle.net/11250/246281`.

[15] J.-P. Gaspard, A. Pellegatti, F. Marinelli and C. Bichara, Peierls instabilities in covalent structures I. Electronic structure, cohesion and the $Z = 8 - N$ rule, *Philos. Mag.* **B77**, 727 (1998), DOI: 10.1080/13642819808214831.

[16] J. Zhang, W. Cui, M. Juda, D. McCammon, R.L. Kelley, S. H. Moseley, C. K. Stahle and A. E. Szymkowiak, Non-Ohmic effects in hopping conduction in doped silicon and germanium between 0.05 and 1 K, *Phys. Rev. B* **57**, 4472 – 4481 (1998), DOI: 10.1103/PhysRevB.57.4472.

[17] J. C. Mather, Bolometer noise: nonequilibrium theory, *Appl. Opt.* **21**, 1125 – 1129 (1982), DOI: 10.1364/AO.21.001125.

[18] S. H. Moseley, J. C. Mather and D. McCammon, Thermal detectors as xray spectrometers, *J. Appl. Phys.* **56**, 1257 – 1262 (1984), DOI: 10.1063/1.334129.

[19] W. A. Little, The transport of heat between dissimilar solids at low temperatures, *Can. J. Phys.* **37**, 334 – 349 (1959), DOI: 10.1139/p59-037.